Molecular Study on Dominant Fatty Acid Esters Characterized from Waste Beef Tallow Biodiesel – A Quantum Computational Approach

Gokul Raghavendra Srinivasan[a], Vijayalakshmi Shankar[a], Ranjitha Jambulingam[a,*]

[a] CO2 Research and Green Technologies Centre, Vellore Institute of Technology, Vellore

*corresponding author: Ranjitha Jambulingam
Email id: ranjitha.j@vit.ac.in

Abstract:

This study deals with computational analysis of dominant fatty acid ethyl esters characterized from the biodiesel produced from waste beef tallow by means of KOH catalyzed ethanol based transesterification. Ethyl palmitate, Ethyl Oleate, Ethyl Stearate and Ethyl Myristate were identified as dominant fatty acid esters and were computed for molecular analysis in Gaussian 09 software using Density Functional Theory (B3LYP method) with 6-31G* as basis set. Geometric parameters were in accordance with existing experimental values and population analysis exhibited negative charge for oxygen atoms, both positive & negative charge for carbon atoms in all ester molecules. The molecular dipole moment was higher for unsaturated ester molecule and quadruple moment proposed electronic dislocation in X+Y direction. Also, energy gap decreased slightly with increasing carbon chain but reduced drastically with increase in unsaturation. Electrostatic potential mapping displayed negative electrostatic potential for oxygen atoms in ester linkage of all ester molecules.

Keyword: beef tallow biodiesel, Fatty Acid Esters, Atomic Charge, molecular dipole moment, HOMO-LUMO energy gap, Electrostatic Potential

Introduction

Biodiesel is regarded as the most promising renewable biofuel serving as an effective replacement for existing petro fuels in both developed and developing countries due to its robustness and remarkable energy density. This eco-friendly fuel has not only satisfied the global energy demand because of overgrowing population but also reduced the potential threats to the environment.

In general, biodiesel is a fatty acid alkyl ester molecule; made up of large carbon chained fatty acid molecule linked with short chained alkyl radical by an ester functional group. It is a highly biodegradable, non-toxic fuel with improvised combustion characteristics and reduced emission characteristics because of absence of sulphur and aromatic content in its molecular structure [1]. Conventionally, biodiesel is produced by transesterifying triglycerides in oil/fat rendered from various feedstocks like: non-edible seeds [2, 3], waste animal fat [4, 5], waste cooking oil [6], and pyrolyzed oil from waste biomass and rubber products [7].

Numerous studies on biodiesel related to its: theoretical and experimental optimization of reaction and its parameters [8], mathematical modeling of reaction and reactors [9], thermal-physicochemical properties [10], comprehensive engine characteristics study [11], unconventional applications like biodegradation of crude oil [12] have been carried out to understand its viability as successful replacement for diesel fuel in terms of global scale commercialization. Interestingly, the

 doi:10.20944/preprints201906.0118.v1

fatty acid esters present in the biodiesel imparts a significant role in deciding its overall thermal & physicochemical properties [13] and engine characteristics [14]. Hence, understanding its molecular and quantum properties would help the researchers to understand its subatomic behavior which holds key for mathematical modeling of its reaction kinetics and combustion chemistry; and this can be achieved by carrying out quantum computational study on biodiesel molecules.

Normally, quantum computational chemistry deals with the study of properties of matter by developing models based on its behavior at subatomic scale and is governed by Schrödinger equation. These models are based on the basic principles of quantum mechanics and are taken to macroscopic scale by means of statistical mechanics [15]. Various approximation techniques are employed for modeling based on the size of molecule being analyzed, availability of computational resources and degree of accuracy. Accordingly, the molecular modeling based on born-opperheimer approximation technique considers the mass of nuclei and electron [16]; meanwhile another approximation technique is based on parameters method, subdivided into semi-empirical method and empirical method where former considers data from previous computations and latter deals with data related to nuclei only [17]. Similarly, hartree-fock approximation aims in finding approximation of ground state electronic wave function [18] whereas for density functional methods, electron density is maintained as the main variable [19]. In addition, different types of basis set like STO-3G, 6-31G,6-31G*,cc-pVNZ (where N=D,T,Q,5…) are used for the computational purpose and represents the mathematical description of orbitals in form of electronic wave function. The basis set used in this study is 6-31G*, representing fixed linear combinations of Gaussian functions which add six d-type Cartesian-Gaussian polarization functions on each atom [20]. Even though, these studies are widely appreciated for determining the reaction pathways, thermal and physical data, only few studies have been carried out regarding quantum computational study on triglycerides and fatty acid ester molecules.

Accordingly, Marton et al.,2010 presented the computational data related to methoxide assisted transesterification of triglyceride in biodiesel production and determined the most probable reaction pathway and most favored intermediates using DFT B3LY/6-31G(d) by correlating the structural parameters of 8 triglyceride molecules. This study proposed that long saturated carbon chains bent towards the unsaturated fatty acid radical and also concluded that the neighboring effect of carboxyl groups and long chain influenced the energies of intermediate products [21]. Likewise, transesterification of triglyceride was considered in terms of activation energy computed using molecular orbital calculations (HF method/ STO-3G) and was found to be different under basic and acidic condition where acid catalyzed reaction was slower than base catalyzed reaction because of larger & more stable cyclic transition state .It was reported that formation of cyclic transition state of Carbon atom ,carboxyl group and reactant is necessary for transesterification and hydrolysis reaction [22]. Supporting this, the reaction pathways of transesterification of Jatropha oil with glycerides of Palmitic acid, oleic acid and linoleic acid were investigated using semi empirical AM1 Molecular orbital calculations and concluded the involvement of 3 important steps in the reaction as follows: step 1- nucleophilic attack of alkoxides anion on carboxyl group (tetrahedral intermediate); step 2- breaking of tetrahedral intermediate to form alkyl ester and glyceride ion and step 3- regeneration of active catalyst , starting another catalytic cycle. In addition, Decomposition of tetrahedral intermediate determines the rate of base catalyzed transesterification [23].

Preprints (www.preprints.org) | NOT PEER-REVIEWED | Posted: 13 June 2019 doi:10.20944/preprints201906.0118.v1

Regarding Fatty acid ester molecules, Jiao et al., 2015 identified methyl butanoate as an ideal substitute for fatty acid ester of biodiesel and studied their thermodynamics and kinetics of auto-ignition chemistry using Composite CBS-QB3 calculations by constructing potential energy profiles of radicals derived from it [24]. Similarly, work carried out by Osmont et al., 2007 helped in determining gas-phase thermodynamic properties at 298.15 K and 300-5000 K range of methyl and ethyl esters of vegetable oil using B3LY/6-31G(d,p) and the predicted value was in accordance until C10 chain, C9-C15 chain were contradictory but beyond C16 data was unique. In addition, the correlated data were found to be highly useful for modeling combustion chemistry, thermal decomposition and oxidation [25]. In addition, Potrich et al., 2018 computed the enthalpy and Gibbs free energy of methyl to pentyl esters formation using B3LY/6-31G(d,p) and group contribution method of Constantinou and Gani (MCG); and proposed that the work was an effective tool for calculating thermodynamic data of esters that are difficult to be synthesized or impossible experimenting [26]. Above all, Gokul et al., 2019 carried out a comprehensive computational study on methyl oleate regarding its geometry, net atomic charges, molecular moments, analysis on molecular orbitals and electrostatic potential using B3LYP/6-31G*and proposed that oxygen atoms belonging to ester functional group exhibited negative atomic charge and displayed higher activity for proton attraction, indicating higher chances for undergoing reaction than compared to other atoms [27]. Even though, numerous studies have been carried out for different fatty acid esters, no comprehensive study on fatty acid ethyl esters have been carried out to understand its quantum properties.

In this present study, a detailed computational study related to the quantum behavior of dominant fatty acid esters characterized from waste beef tallow have been carried out and have been studied for its geometry, net atomic charges, molecular moments, analysis on molecular orbitals and electrostatic potential using DFT/B3LYP method by maintaining 6-31G*as basis set using Gaussian 09 Software.

Material & Methodology

Production of biodiesel:

Waste beef tallow was rendered from discarded fleshing and slaughterhouse wastes using dry rendering technique. The rendered tallow was refined by filtration, successive water washing, dehydrating at 110^{O}C followed by degumming using orthophosphoric acid to remove phospholipids [28]. The refined tallow was subjected for ethanol based transesterification by maintaining catalyst concentration as 0.5% KOH, reaction time and temperature as 120 minutes and 60^{O}C. Post reaction, biodiesel was separated from glycerol by decantation followed by progressive waster washing and drying thoroughly.

Identification of dominant fatty acid esters:

Beef tallow biodiesel was prepared for GC-MS analysis as per American testing standard-ASTM 2256. The fatty acid esters were identified based on the peak obtained at its corresponding retention time whereas their availability were decided based on the intensity of the peak. Figure 1 depicts the Gas chromatographic spectra of waste beef tallow biodiesel.

Insert Figure 1 here

Preprints (www.preprints.org) | NOT PEER-REVIEWED | Posted: 13 June 2019 doi:10.20944/preprints201906.0118.v1

Computational analysis of Dominant ester:

The computational calculations were performed for identified dominant fatty acid esters using Density functional theory at 6-31G* level for B3LYP method in Gaussian 09 software [29]; which performs calculations relevant to electronic structures using molecular structure as input in Cartesian coordinates based on Schrödinger equation (Equation 1).

$$\frac{\hbar^2}{2m}\nabla^2\Psi(\mathrm{r}) + V(r)\,\Psi(\mathrm{r}) = \mathrm{E}\Psi(\mathrm{r}) \qquad \text{Equation 1}$$

Here, Equation 1 combines exact Hartree-Fock exchange with local and gradient correct exchange and other correlation associated with it. Similarly, the exchange correlation functional verified by Becke, 1986 is given in Equation 2 [30].

$$E_{XC} = (1 - a_o)E_X^{LSPA} + a_o E_X^{HF} + \Delta E_X^{B88} + E_C^{LSDA}\, a_c \Delta E_C^{PW91} \qquad \text{Equation 2}$$

, where ΔE_X^{B88} is becke's gradient correction to exchange functional whereas ΔE_C^{PW91} is Perdew-Wang gradient correction to correlational function [31].

For computational purpose, Optimization method was used to compute the geometric parameters like bond length, bond angle whereas the charge transfer within the molecule and its chemical potential were defined based on the analyses carried out on Molecular orbitals and their kinetic energies. Similarly, molecular moment calculations helped in determining the electrostatic moment due to charge distribution while electrostatic potential mapping and electron charges briefed about the interactions of molecules with each other or molecular interactions with other molecules.

Result and Discussions:

Based on past literatures and previous study [27], the average molecular weight of beef tallow was calculated based on the composition of its fatty acids with help of Equation 3 [3] and was found to be 850.92 g/mol.

$$\mathrm{M(TG)}=92.09 - 3 + 3[\mathrm{M(HA)} - 17] \qquad \text{equation 3}$$

For stoichiometry, the molar ratio was calculated between the tallow and ethanol and was found to be optimum for 1:6 (tallow: ethanol). Based on optimized transesterification reaction, maximum yield of 96% was achieved. Here, the reaction temperature was maintained considering the boiling point of ethanol and melting point of tallow.

Based on GC spectra, ethyl palmitate, ethyl oleate, ethyl stearate, ethyl myristate were identified as dominant fatty acid esters in a composition of 37.36%, 25.17%, 14.78% and 13.79%. Since dominant Fatty acid esters influence the properties and engine characteristics of resultant biodiesel, computational analysis related to molecular geometry, net atomic charges and moment calculations, electrostatic potential mapping, molecular orbital analysis were performed for these ester molecules.

Optimization of geometrical parameters

Geometrical optimization technique uses wave function and energy difference in geometries at initial and lowest energy level of a molecule for calculating its minimum energy configuration. The

 doi:10.20944/preprints201906.0118.v1

optimized geometrical properties like bond length, bond angle were computed using DFT method (B3LYP/6-31G*). Table 1-2 summarizes the calculated bond length and bond angle between the important bonds of dominant fatty acid ester molecules. From table 1, it was clearly concluded that the average bond length of C-C bond for all ester molecules were found to be 1.53Å, whereas in case of C=C bond in ethyl stearate, it was found to be 1.34Å. Also, the bond length between C and H was found to be 1.11Å for all fatty acid ester molecules. In addition, the bond length between C-O and C=O corresponding to ester functional group were calculated as 1.44Å and 1.21Å respectively. Surprisingly, contraction in bond length of C-C band at carbon atoms adjacent to functional group and unsaturated bond (C9-C10), in case of ethyl oleate, was because of electronegativity equalization which distributes electron according to Mullikan electronegativity, thereby adjusting the bond length accordingly [32] (Figure 2). From figure 3, it can be concluded that saturated Fatty acid esters possessed linear carbon chain whereas unsaturated fatty acid esters had non-linear structure owing to the SP2 carbons giving rise to trigonal planar instead of tetrahedral structure [33]. Similarly, the bond angle between the saturated carbon atoms were found to be 113^{O} representing the tetrahedral values whereas for unsaturated carbon atoms, it was found to be 125^{O}, representing trigonal values. Eventually, all the geometric values were found to be in good accordance with the actual range [34] and acts as the base data for computing advanced calculations including vibrational momentums.

Insert Table 1 here

Insert Figure 2 here

Insert Table 2 here

Insert Figure 3 here

Net atomic charges

In general, molecular dipole moment and atomic charges are calculated using valence and multipolar population coefficient [35] but are calculated theoretically based on the charges obtained from Natural Population analysis (NPA) using B3LYP method with 6-31G* as basis set.

Based on population analysis, oxygen atoms in the ester linkage of fatty acid ester molecules exhibited negative atomic charges whereas carbon atoms bonded with it exhibited positive atomic charges. The net negative charge of the oxygen atom was because of its higher electronegativity which tends to pull the shared electrons towards itself thereby giving positive charges to the carbon atoms. However, in case of carbon atoms in fatty acid chain, positive charge was a resultant of carbocation formation upon losing electron during H bond formation whereas negative charge was because of carboanion formation upon gaining electron during hydrogen bonding. Likewise, hydrogen atom in all fatty acid ester molecules exhibited positive charges. Table 2 consolidates the Mullikan atomic charges of hydrogen summed up carbon atoms and oxygen atoms of different fatty acid esters computed based on the population analysis. Figure 4 illustrates the atomic charges of summed up carbon atoms and oxygen atoms as graphical representation in form of histogram.

Insert Table 3 here

Insert Figure 4 here

Preprints (www.preprints.org) | NOT PEER-REVIEWED | Posted: 13 June 2019 doi:10.20944/preprints201906.0118.v1

Molecular moments:

In general, moments due to charge distribution and electrostatic field gradient are determined by correlating density function with average value of quantum observable ⟨O⟩. The relationship between density function and quantum observable ⟨O⟩ is correlated in equation 4:

$$\langle O\rangle = \int_V \hat{O}(\vec{r})\rho(\vec{r})d\vec{r} \qquad \text{Equation 4}$$

Upon replacing ρ with ∇ρ, electrostatic moment can be determined. The components of molecular dipole and quadruple moment of fatty acid esters were determined using B3LYP method with 6-31G* as basis set. Since the center of mass of fatty acid ester molecules coincided with the origin, their corresponding inertial axis was considered as their Cartesian system.

Similarly, components corresponding to electrostatic quadruple moment can be calculated by replacing ⟨O⟩ with $\overrightarrow{r_\alpha} \wedge \overrightarrow{r_\beta}$ and density function with multipolar expansion to order l=1 in equation 4. The modified equation for determining components of quadruple moment is represented in Equation 5 [36].

$$Q_{\alpha\beta} = \sum[\, Q^i_{\alpha\beta} + r_{i\beta}d_{i\alpha} + r_{i\alpha}d_{i\beta} + r_{i\beta}r_{i\alpha}q_i] \qquad \text{Equation 5}$$

Upon integrating equation 4, without considering multipolar expansion, we get equation 6 and 7,

$$Q_{\alpha\beta} = \frac{1}{V}\sum_{\vec{H}} \Delta F(\overrightarrow{H}) \left[\sum_i (\, Q^i_{\alpha\beta} + r_{i\beta}d_{i\alpha} + r_{i\alpha}d_{i\beta} + r_{i\beta}r_{i\alpha}q_i)\right] \qquad \text{Equation 6}$$

$$Q^i_{\alpha\beta} = \int_{ti} (\, r_\alpha - r_i)\,(r_\beta - r_i) e^{i2\pi\vec{H}\,(\vec{r}-\vec{r_i})} d^3r \qquad \text{equation 7}$$

Where, Summation over $\vec{H}$, performed for all structure factors Indices and t_i represents the integral subunits

Table 4 summarizes the molecular dipole and quadruple moment of dominant fatty acid esters determined based on the analysis carried using Density Functional Theory (DFT) method at B3LYP level keeping 6-31G* as basis set. From table, it was clearly noticed that there was a slight reduction in dipole moment with increase in carbon chain length which dilutes the dipole and reduces the intermolecular attraction; however higher dipole moment for ethyl stearate was because of its nonlinear structure due to the presence of unsaturated double bond [37]. Similarly, the quadruple moment was found to acting in X+Y direction for all esters owing to the linearity in the molecular structure. Unlike, dipole moment, quadruple moment increased with carbon chain length. However, the quadruple moment calculated based on DFT method exhibited weaker charge expansion for all fatty acid esters.

Insert Table 4 here

Frontier molecular orbital analysis:

In general, molecular orbitals help in predicting the highly reactive position in π-electron system based on frontier electron density [38]. The Highest occupied molecular orbitals (HOMO) and lowest unoccupied molecular orbitals (LUMO) energy separation helps in characterizing conjugate molecules and influences its chemical stability based on the difference in this energy level called

Preprints (www.preprints.org) | NOT PEER-REVIEWED | Posted: 13 June 2019 doi:10.20944/preprints201906.0118.v1

energy gap. Also, HOMO and LUMO defines the ability of molecule to donate or accept electron respectively. Similarly, these orbitals describes about the transition of electron from ground state to its first excited state when it jumps from Highest occupied molecular orbitals (HOMO) to lowest unoccupied molecular orbitals (LUMO); and also decides the atom's ionization potential (using HOMO) and its electron affinity (using LUMO).

The orbital energies of Highest occupied molecular orbitals (HOMO) and lowest unoccupied molecular orbitals (LUMO) of dominant fatty acid esters were computed using Density Functional Theory (DFT) method at B3LYP level keeping 6-31G* as basis set and are summarized in Table 5. It was clearly evident that energy gap between HOMO and LUMO decreased slightly with increase in carbon chain length but decreased drastically in case of increase in unsaturation. This reduced energy gap (0.23102 a.u. or 6.28 eV) in ethyl oleate makes it slightly less stable and likely more reactive than compared to other saturated fatty acid esters. In addition, it can be noted that the energy gap of ethyl palmitate and ethyl stearate were almost identical (0.2667 a.u or 7.25 eV), hence it can be concluded that they tends to exhibit similar stability and reactivity [39].

Insert Table 5 here

Electrostatic potential

Molecular electrostatic potential is a potential experienced, due to distribution of electron density, by unit positive charge at any point surrounding the molecule and helps in predicting sites of electrophilic attack (positive potential) , nucleophilic attack and protonation (negative potential). The molecular electrostatic potential distribution can be calculated using equation 8.

$$\phi(r)=\int \frac{\rho_{total}(r)}{|(r-r')|}d \qquad \text{Equation 8}$$

where, ρ_{total} denotes nuclear and electronic charge; and is integrated over volume. The fatty acid esters were mapped with electrostatic potential map based on the energy analysis carried out using Density Functional Theory (DFT) method at B3LYP level keeping 6-31G* as basis set. Figure 5 illustrates the electrostatic potential mapping of dominant fatty acid esters. All fatty acid ester molecules exhibited positive electrostatic potential for C-H bonds while C-O and C=O bonds exhibited negative electrostatic potential. The negative electrostatic potential for C-O and C=O bonds was because of its concentrated electron density which tends to attract proton towards itself. Accordingly, highest negative electrostatic potential was noted for single bonded oxygen atom (O2) followed by double bonded oxygen atom (O1) for all fatty acid ester molecules. Figure 6 illustrates the electron density maps of dominant fatty acid esters at ester linkage.

Insert Figure 5 here

Insert Figure 6 here

Conclusions:

Thus the computational analysis on dominant fatty acid esters were successfully carried out in Gaussian 09 software using Density Functional Theory (B3LYP/6-31G*). The following were the conclusions drawn based on this computational study on these ester molecules.

(i) The bond length and Bond angle computed using geometrical optimization were in accordance with the results from previous literatures determined experimentally and theoretically.

(ii) Based on population analysis, carbon atoms exhibited both positive and negative charges; hydrogen atoms exhibited only positive charges. Meanwhile, oxygen atoms in ester linkage exhibited negative atomic charge due to its high electronegativity. In addition, this higher electronegativity imparted negative electrostatic potential for the molecule making its prone for proton attack and was found to be higher for C-O bond followed by C=O bond.

(iii) The energy gap between HOMO-LUMO decreased slightly with increase in carbon chain length but decreased drastically in case of increase in unsaturation, thus explaining the higher reactivity and less stability of ethyl oleate.

(iv) The molecular dipole moment was higher for saturated fatty acid esters and quadruple moment was found to be acting in X-Y direction for all ester molecules.

These computational analyses on molecular behavior helps in providing fundamental data of these molecules which can be used for numerous calculations related to its combustion chemistry and properties.

Conflict of Interest:

The author(s) wish to declare that there are no potential conflicts of interest with respect to the research, authorship, and/or publication of this article.

References:

1. Srinivasan, G.R. and Jambulingam, R. *Journal of Environmental Science and Technology*.**2018**, *11,157*-166.
2. Demirbas, A. *Energy Sources, Part B*. **2009**, *4*(3), 310-314.
3. Srinivasan, G.R.; Palani, S. and Ranjitha, J. *Innovative Energy and Research*.**2017**, *6*(2), 165.
4. Banković-Ilić, I.B.; Stojković, I.J.; Stamenković, O.S.; Veljkovic, V.B. and Hung, Y.T. *Renewable and sustainable energy reviews*.**2014**, *32,238*-254.
5. Srinivasan, G.R.; Palani, S. and Jambulingam, Ranjitha. *Journal of Engineering Science and Technology*.**2018**, *13*(8), 2632-2643.
6. Kawentar, W.A. and Budiman, A.*Energy Procedia*.**2013**, *32,190*-199.
7. Arbogast, S.; Bellman, D.;Paynter, J.D. and Wykowski, J. *Fuel processing technology*. **2013**,*106*,518-525.
8. Singh, G.; Mohapatra, S.K.; S. Ragit, S. and Kundu, K. *Energy Sources, Part A: Recovery, Utilization, and Environmental Effects*.**2018**, *40*(18), 2144-2153.
9. Silva, M.G.; Nobre, L.R.; Santiago, L.E.; Deus, M.S.; Jesus, A.A.; Oliveira, J.A. and Souza, D.F. *Energy & fuels*.**2018**, *32*(9), 9614-9623.
10. Barabás, I. and Todoruț, I.A.*Intechopen, Rijeka.2011, 3*-28.
11. Senthilkumar, G.; Sajin, J.B.; Yuvarajan, D. and Arunkumar, T. *Environmental technology*. **2018**, 1-8.
12. Palani, S.; Srinivasan, G.R. and Jambulingam, R.*J Earth Sci Clim Change*. **2018**, *9*(2).
13. Jambulingam, R. and Srinivasan, G.R. *ICRDME 2K19 conference proceedings*. **2019**.

14. Srinivasan, G.R.; Shankar, V. and Jambulingam, R. *Energy Exploration & Exploitation*.**2019**, 1-27.
15. Cook, D.B. *Handbook of computational quantum chemistry*. Courier Corporation.**2005.**
16. Combes, J.M.; Duclos, P. and Seiler, R.Springer, Boston, MA.**1981**, 185-213
17. Ramachandran, K.I.; Gopakumar, D. and Namboori, K.*Computational Chemistry and Molecular Modeling: Principles and Applications*.**2008**, 139-154.
18. Fischer, C.F. Hartree--Fock method for atoms. A numerical approach. **1977**
19. Harrison, N.M. *Nato Science Series Sub Series III Computer and Systems Sciences*.**2003**, *187*, 45-70.
20. Rassolov, V.A.; Pople, J.A.; Ratner, M.A. and Windus, T.L.*The Journal of chemical physics*.**1998**, *109*(4), 1223-1229.
21. Marton, G.; Pleşu, V.; Marton, A. and Bercaru, M.T. 2010. *Chemical Engineering*.**2010**, *21*,1351-1356.
22. Asakuma, Y.; Maeda, K.; Kuramochi, H. and Fukui, K. *Fuel*.**2009**, *88*(5), pp.786-791.
23. Tapanes, N.C.O.; Aranda, D.A.G.; de Mesquita Carneiro, J.W. and Antunes, O.A.C. *Fuel*. **2008**, *87*(10-11), 2286-2295.
24. Jiao, Y.; Zhang, F. and Dibble, T.S. *The Journal of Physical Chemistry A*. **2015**, *119*(28), 7282-7292.
25. Osmont, A.; Catoire, L. and Gökalp, I.*International Journal of Chemical Kinetics*. **2007**, *39*(9), 481-491.
26. Potrich, E.; Voll, F.A.P.; Cabral, V.F. and Filho, L.C. *Chemical Industry and Chemical Engineering Quarterly.* **2019***, 28.*
27. Gokul, R.S. and Jambulingam, R. *Research Journal of Chemistry and Environment.***2019***, 23*, (2),51-59.
28. Srinivasan, G.R.; Palani, S. and Jambulingam, R.*Journal of Biofuels*.**2018**, *9*(1), 17-24.
29. Gaussian 09, Revision A.1, Gaussian, Inc., Wallingford CT. **2009.**
30. Becke, A.D. *The Journal of Chemical Physics*.**1986**, *84*(8), 4524-4529.
31. Perdew, J.P. and Wang, Y. *Physical Review B*.**1992**, *46*(20), p.12947.
32. Rick, S.W.; Stuart. Reviews in computational chemistry. Wiley.**2002**, 106
33. Ramírez-Verduzco, L.F.; Rodríguez-Rodríguez, J.E. and del Rayo Jaramillo-Jacob, A. *Fuel*.**2012**, *91*(1), 102-111.
34. Heyrovsk, R. *arXiv:0804.4086 [physics.gen.ph]*. **2008.**
35. Jeffrey, G.A.; Cruickshank, D.W.J. and Cox, E.G.*Quarterly Reviews, Chemical Society*. **1953**, *7*(4), 335-376.
36. Drissi, M.; Benhalima, N.; Megrouss, Y.; Rachida, R.; Chouaih, A. and Hamzaoui, F.*Molecules* .**2015**, *20*(3), 4042-4054.
37. Lewis, G.L. and Smyth, C.P. *Journal of the American Chemical Society***. 1940**, *62*(6), 1529-1533.
38. Choi, C.H. and Kertesz, M. *The Journal of Physical Chemistry A*. **1997**, *101*(20), 3823-3831.
39. Ituen, E.B., Akpan, I.J. and Oluwaseyi, O.R.*Int'l. Organization of Scientific Research, J. App. Chem.***2014**, *7*(5), 8-12.

Preprints (www.preprints.org) | NOT PEER-REVIEWED | Posted: 13 June 2019 doi:10.20944/preprints201906.0118.v1

List of Tables

Table 1: calculated bond length of important bonds in fatty acid ester molecules

Atom 1	Atom 2	Ethyl Myristate	Ethyl Palmitate	Ethyl Stearate	Ethyl Oleate
		n=14	n=16	n=18	n=18
C1	C2	1.53766	1.53711	1.53713	1.53706
C2	C3	1.53975	1.53976	1.53977	1.53973
C3	C4	1.53927	1.53923	1.53924	1.53929
C4	C5	1.53934	1.53937	1.53939	1.53945
C5	C6	1.53933	1.53934	1.53935	1.53935
C6	C7	1.53933	1.53933	1.53934	1.53801
C7	C8	1.53934	1.53933	1.53934	1.53998
C8	C9	1.53933	1.53933	1.53934	1.51437
C9	C10	1.53939	1.53933	1.53934	1.34177
C10	C11	1.53933	1.53935	1.53935	1.51433
C11	C12	1.53926	1.53921	1.53934	1.54005
C12	C13	1.53486	1.53917	1.53936	1.53829
C13	C14	1.51013	1.53835	1.53922	1.53924
C14	C15	-	1.53386	1.53918	1.53953
C15	C16	-	1.50976	1.53836	1.53855
C16	C17	-	-	1.53387	1.53443
C17	C18	-	-	1.50974	1.51025
Cn	O1	1.23723	1.23626	1.23627	1.23636
Cn	O2	1.37689	1.37829	1.37826	1.37711
O2	C'1	1.47332	1.48009	1.4799	1.48181
C'1	C'2	1.5188	1.51739	1.51741	1.51715

Preprints (www.preprints.org) | NOT PEER-REVIEWED | Posted: 13 June 2019 doi:10.20944/preprints201906.0118.v1

Table 2: Calculated bond angle of important bonds in fatty acid ester molecules

Atom 1	Atom 2	Atom 3	Ethyl Myristate	Ethyl Palmitate	Ethyl Stearate	Ethyl Oleate
			n=14	n=16	n=18	n=18
C1	C2	C3	113.163	113.137	113.138	113.149
C2	C3	C4	113.559	113.53	113.5533	113.536
C3	C4	C5	113.525	113.493	113.495	113.403
C4	C5	C6	113.54	113.504	113.507	113.574
C5	C6	C7	113.517	113.477	113.479	113.3
C6	C7	C8	113.528	113.495	113.5	113.593
C7	C8	C9	113.501	113.475	113.479	113.126
C8	C9	C10	113.476	113.485	113.495	125.228
C9	C10	C11	113.45	113.466	113.478	125.198
C10	C11	C12	113.129	113.444	113.486	113.107
C11	C12	C13	112.545	113.42	113.469	113.564
C12	C13	C14	113.329	113.089	113.445	113.154
C13	C14	C15	-	112.537	113.422	113.55
C14	C15	C16	-	113.255	113.089	112.874
C15	C16	C17	-	-	112.537	112.641
C16	C17	C18	-	-	113.254	113.163
Cn-1	Cn	O1	126.466	126.317	126.315	126.179
O1	Cn	O2	122.488	122.613	122.613	122.59
Cn	O2	C'1	117.505	117.182	117.187	117.15
O2	C'1	C'2	107.032	106.751	106.754	106.753

Preprints (www.preprints.org) | NOT PEER-REVIEWED | Posted: 13 June 2019 doi:10.20944/preprints201906.0118.v1

Table 3: Mulliken charges for summed up carbon and oxygen atoms in fatty acid ester molecules

Atom	Ethyl Myristate	Ethyl Palmitate	Ethyl Stearate	Ethyl Oleate
	n=14	n=16	n=18	n=18
C1	-0.016923	0.008348	0.008357	-0.016558
C2	0.006891	0.00168	0.00159	0.006669
C3	0.008357	-0.000085	-0.000106	0.008966
C4	0.001869	0.000703	0.000502	0.001873
C5	-0.000078	0.000083	0.000069	0.000981
C6	0.001219	0.001063	0.000528	-0.000375
C7	0.000203	0.000116	0.000011	0.000171
C8	0.002566	0.002509	0.001009	-0.011082
C9	0.000867	0.000838	0.00671	0.010261
C10	0.008673	0.008664	-0.01703	0.010144
C11	-0.006102	-0.006116	0.000084	-0.010799
C12	0.064406	0.0644	0.002505	0.002173
C13	0.01058	0.010549	0.000852	0.000376
C14	0.522969	-0.016999	0.008657	0.009491
C15	-	0.006771	-0.006141	-0.0056
C16	-	0.522975	0.064394	0.064728
C17	-	-	0.010555	0.010759
C18	-	-	0.522964	0.522907
O1	-0.425034	-0.425056	-0.425063	-0.424885
O2	-0.511253	-0.511275	-0.511249	-0.511208
C'1	0.300827	0.300859	0.30084	0.300921
C'2	0.029965	0.029971	0.029962	0.030086

Preprints (www.preprints.org) | NOT PEER-REVIEWED | Posted: 13 June 2019 doi:10.20944/preprints201906.0118.v1

Table 4: Components of molecular dipole and quadruple moments of fatty acid ester molecules

	Ethyl Myristate	Ethyl Palmitate	Ethyl Stearate	Ethyl Oleate
Molecular Dipole Moment				
X	0.3878	0.3888	0.3896	-0.0995
Y	-1.6882	-1.6873	-1.6862	2.0179
Z	0.0003	0.0002	0.0001	0.0002
Total	1.7321	1.7315	1.7306	2.0204
Molecular Quadruple Moment				
XX	-107.5727	-120.7178	-133.8795	-138.7937
YY	-123.9288	-137.5379	-151.1505	-146.2526
ZZ	-113.4279	-126.4657	-139.5024	-139.1709
XY	-9.7216	-11.9022	-14.0795	16.1682
XZ	-0.001	-0.0078	-0.0071	0.0018
YZ	0.0003	0.0023	0.0034	-0.002

Table 5: Orbital energies at HOMO and LUMO; energy gap for fatty acid esters

Orbital Type	Ethyl Myristate		Ethyl Palmitate		Ethyl Stearate		Ethyl Oleate	
	orbital	Orbital Energies (a.u.)	orbital	Orbital Energies(a.u.)	orbital	Orbital Energies (a.u.)	orbital	Orbital Energies (a.u.)
LUMO	73	0.00146	81	0.00164	89	0.00164	88	0.00139
HOMO	72	-0.26852	80	-0.26838	88	-0.26837	87	-0.23241
Energy Gap	**0.26706 a.u.**		**0.26674 a.u.**		**0.26673 a.u.**		**0.23102 a.u.**	

Preprints (www.preprints.org) | NOT PEER-REVIEWED | Posted: 13 June 2019 doi:10.20944/preprints201906.0118.v1

List of Figures

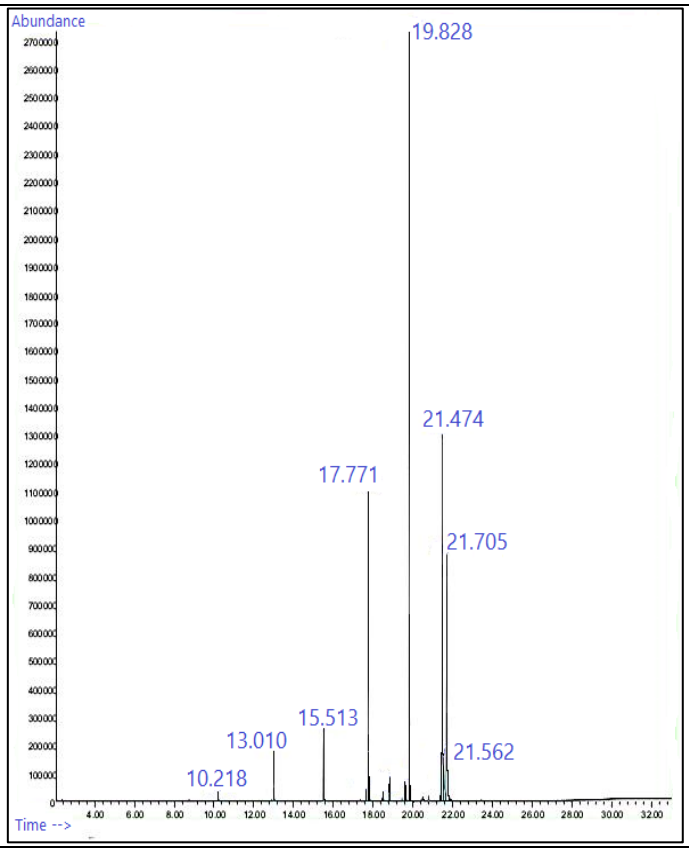

Figure 1: GC spectra of beef tallow biodiesel

Preprints (www.preprints.org) | NOT PEER-REVIEWED | Posted: 13 June 2019 doi:10.20944/preprints201906.0118.v1

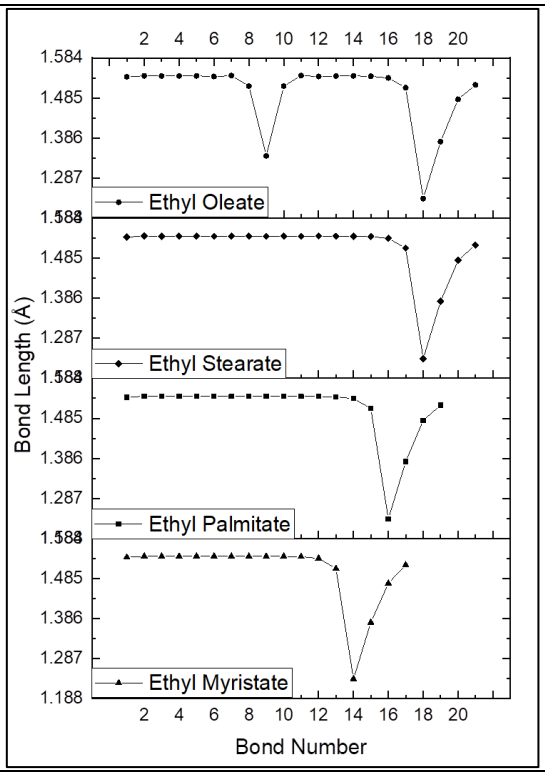

Figure 2: Bond length of carbon chain for different ester molecules

Preprints (www.preprints.org) | NOT PEER-REVIEWED | Posted: 13 June 2019 doi:10.20944/preprints201906.0118.v1

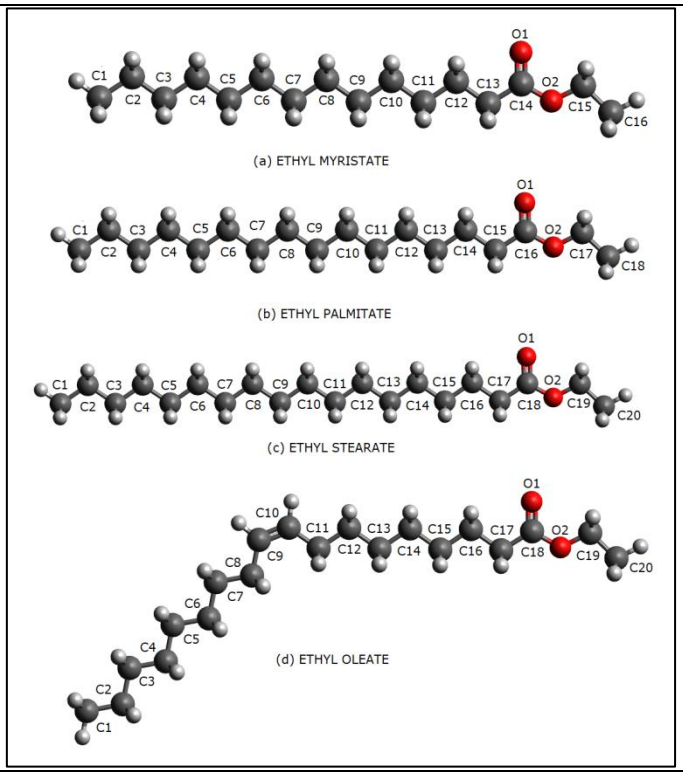

Figure 3: Optimized 3D molecular structure of (a) ethyl myristate; (b) ethyl palmitate; (c) ethyl stearate and (d) ethyl oleate

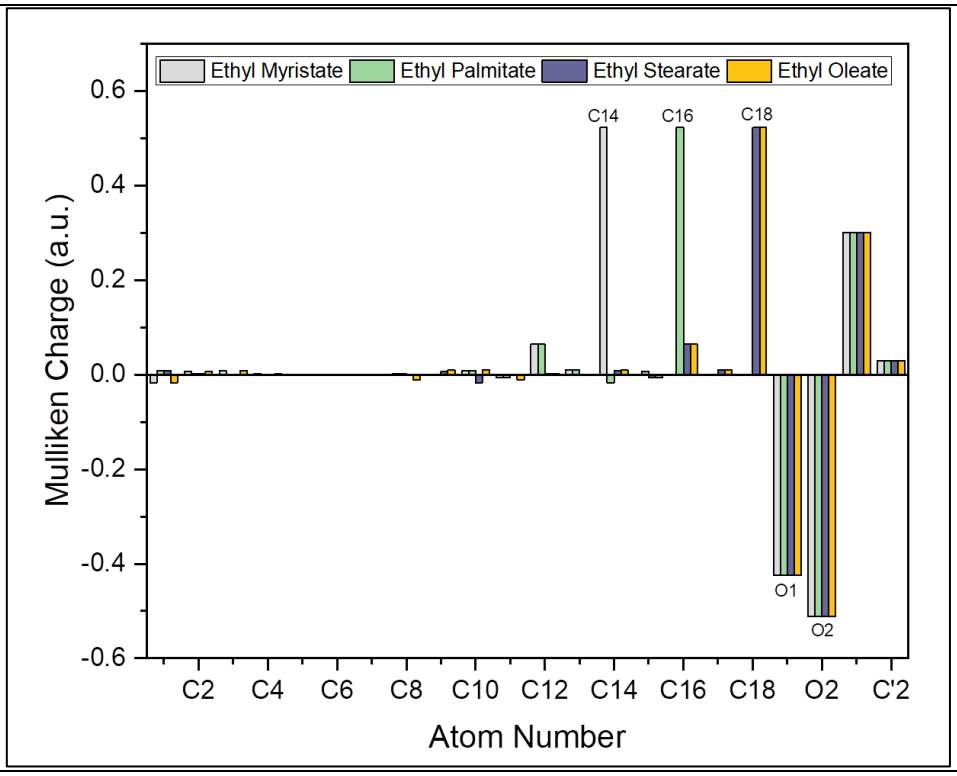

Figure 4: Histogram of atomic charges of summed up carbon and oxygen atoms in fatty acid ester molecules

Preprints (www.preprints.org) | NOT PEER-REVIEWED | Posted: 13 June 2019 doi:10.20944/preprints201906.0118.v1

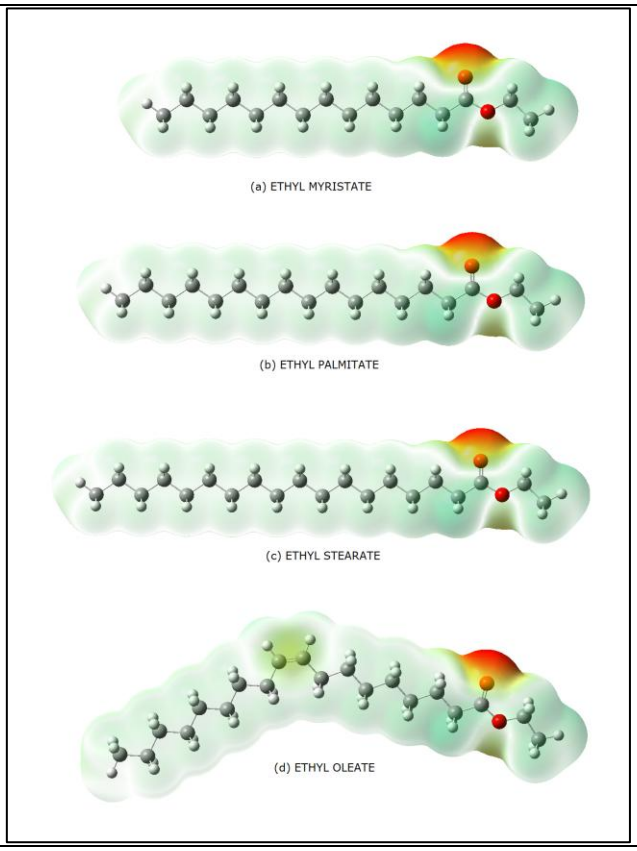

Figure 5: Electrostatic potential mapping of (a) ethyl myristate; (b) ethyl palmitate; (c) ethyl stearate and (d) ethyl oleate

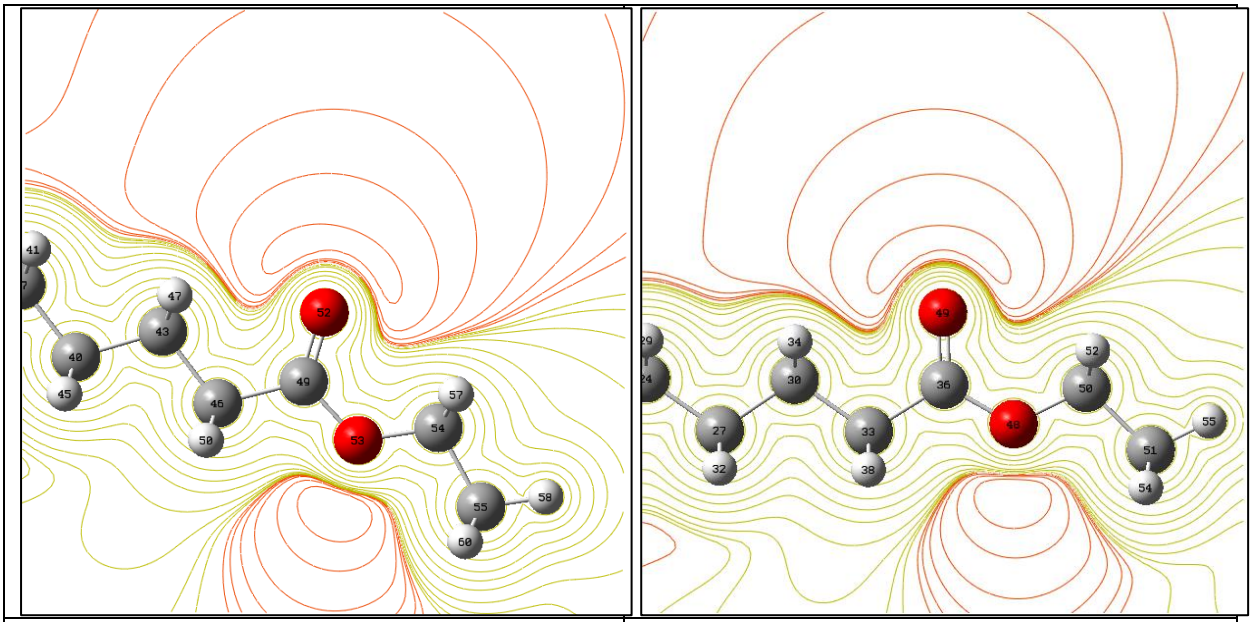

(a) ETHYL MYRISTATE (b) ETHYL PALMITATE

Preprints (www.preprints.org) | NOT PEER-REVIEWED | Posted: 13 June 2019 doi:10.20944/preprints201906.0118.v1

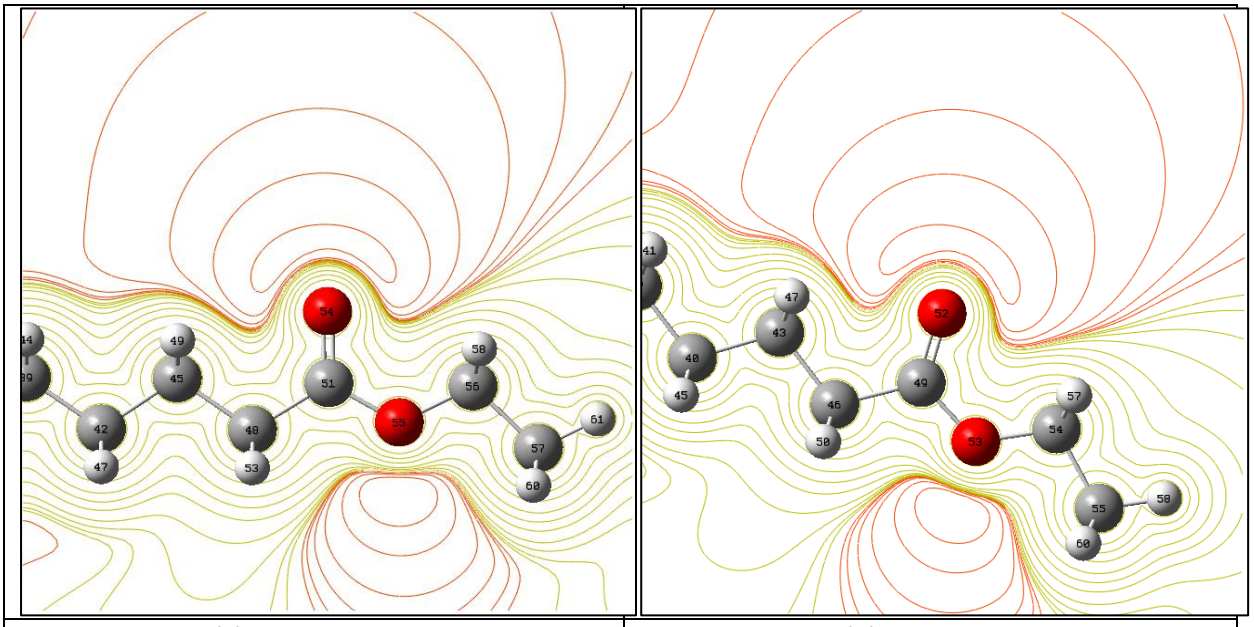

(c) ETHYL STEARATE | (d) ETHYL OLEATE

Figure 6: Electron density mapping at ester linkage of (a) ethyl myristate; (b) ethyl palmitate; (c) ethyl stearate and (d) ethyl oleate